ORIGINAL PAPER

Understanding the limits to the hydraulic leg mechanism: the effects of speed and size on limb kinematics in vagrant arachnids

Charlotte Boehm[1] · Johanna Schultz[1,2] · Christofer Clemente[1]

Abstract

Among invertebrates, spiders (order Araneae) may be unique in their relationship between speed and mass as they use a combination of direct muscular contractions to flex their appendages, and internally controlled hydraulic pressure to extend them. To explore this, we measured maximal running speeds in 128 individual lycosids and sparassids, which varied in mass between 0.0054 and 3.01 g. We show maximum speed scaled with $M^{0.353}$, while mean running speed scaled much lower as $M^{0.197}$. We show no strong limitation of the hydraulic mechanism, with leg extension speed being equal to or greater than leg flexion speed. The reduction in leg flexion speed, only apparent in the distal most joint of the limb, might be a result of the requirement for flexor muscles to act against the hydraulic system. We explored the role of the limbs and found an alternating pattern of joint use among limbs, which may represent a strategy to avoid interference with adjacent limbs during running. Furthermore, we observed a reduced movement speed (increased leg dragging) in the rearward facing fourth limb with size. This may be linked to the increased size of the abdomen in larger spiders and may suggest a speed limitation in larger individuals.

Keywords Sparassidae · Lycosidae · Kinematics · Scaling

Introduction

For many animals, speed is an important and ecologically relevant performance variable as organisms need to move quickly to catch prey, escape from predators, find mates, or defend territories (Garland and Losos 1994). Across many animal taxa, body mass has been identified as a key determinate of speed, following a power-law relationship (Hedenström 2003; Peters 1986).

Most of these studies focused on vertebrates, especially mammals, reptiles, and birds (Bejan and Marden 2006; Clemente et al. 2009; Iriarte-Díaz 2002; Pennycuick 1997; Van Damme and Vanhooydonck 2001). Among mammals, the relationship between speeds at the trot/gallop transition scaled with $Mass^{0.24}$ (Heglund et al. 1974), while the maximal running speed among mammals was later reported to

scale among mammals as $Mass^{0.17}$ (Garland 1983). Maximal running speed among 94 species of lizards showed an exponent for ordinary least-squares regression of $Mass^{0.18}$ (Van Damme and Vanhooydonck 2001), while among 18 monitor lizard species maximal running speed scaled as $Mass^{0.166}$ (Clemente et al. 2009). Yet, studies on the scaling of speed among invertebrates are less common.

Hirt et al. studied speed among invertebrates while freely moving around their environment (exploratory speed) (Hirt et al. 2017). They found reasonable agreement with vertebrates, reporting that the scaling of speed among 57 species of invertebrate scaled with $Mass^{0.19}$. However, they also show that the scaling exponent varied substantially between the taxonomic groups. Insecta tended to follow this pattern scaling as $Mass^{0.19}$, while Diplopoda (millipedes) and Entognatha (e.g., Springtails) scaled lower as $Mass^{0.12}$ and $Mass^{0.07}$, respectively. Furthermore, Malacostraca (e.g., Woodlice), Chilopoda (Centipedes), and Arachnida (Spiders and pseudoscorpions) scaled higher than average as $Mass^{0.47}$, $Mass^{0.53}$, and $Mass^{0.43}$, respectively, suggesting much more variation in the scaling of speed than previously shown (Hirt et al. 2017).

✉ Christofer Clemente
cclement@usc.edu.au

1 School of Science and Engineering, University of the Sunshine Coast, Sippy Downs, QLD, Australia

2 The Robotics and Autonomous Systems Group, CSIRO Data61, Brisbane, QLD, Australia

Yet even among invertebrates arachnids may be unique in their relationship between speed and mass. In contrast to most animals, spiders (order Araneae) do not only use direct muscular contractions to extend their appendages (Biewener and Daniel 2010; Spagna et al. 2011) as they lack extensor muscles in two of the major leg joints, the femur-patella and tibia-metatarsus (Anderson and Prestwich 1975; Ellis 1944; Petrunkevitch 1909). Locomotion is achieved by changes in internal hydraulic pressure (Ellis 1944; Weihmann et al. 2012) where pressure in the cephalothorax/prosoma generates a flow of the hemolymph into the appendages. Spaces between the soft tissues within the leg joints, called lacunae, expand because of this flow of hemolymph, resulting in extension of the legs (Blickhan and Barth 1985; Weihmann 2013). The three main joints participating in leg extension are the trochanter–femur joint, causing a femoral depression towards the substrate with extensor muscles, and the femur–patella and the tibia–metatarsal joint, increasing the ventral joint angle through hydraulic extension (Fig. 1a, orange and blue dots, respectively) (Gasparetto et al. 2008; Weihmann et al. 2012). This variation in the locomotor system may become more important at high speeds, and at larger body masses where the geometric scaling of body shape might limit this unique limb extension system (Bohmann and Blickhan 1998). This may also be evident with the role of the different legs during locomotion.

The limbs of spiders are arranged in a radial pattern around the body, with the front and second limbs directed anteriorly, the third limbs directed medially, and the hind limbs directed posteriorly. Given this arrangement, it is likely that different mechanisms are responsible for propulsion in different limbs. The first and second limbs are likely to flex to contribute to propulsion, while the third limbs both flex and extend at the proximal joint to provide propulsion, as flexion and extension in this leg pair are small (Ehlers 1939; Ward and Humphreys 1981; Weihmann 2013; Weihmann et al. 2012). The hindlimb, with its rearward orientation, extends by increasing ventral joint angles of the femur–patella and the tibia–metatarsus joints, and thereby appear to be the only limbs which mostly rely on the hydraulic mechanism to propel spiders forward (Ellis 1944). Yet, a more recent analysis of force vectors in accelerating spiders suggests that muscular proximal joints may also be important in the hind limbs (Weihmann et al. 2012).

To understand if this limb extension mechanism limits speed, and if non-geometric modifications are required to compensate for it, we explore the locomotion among two groups of spiders with size. We explore maximum speed with size among the ground-based wolf spiders (Lycosidae), and the semi-arboreal huntsmen (Sparassidae). We further explore the role of different limbs with size and speed. Finally, we explore how the length and volume of limb segments changes with size.

Materials and methods

Study animals

In this study, 128 spiders from two spider families, the Lycosidae (*Tasmanicosa godeffroyi*; $N = 71$) and Sparassidae (*Heteropoda jugulans* or *H. cervina*; $N = 57$), were collected. All specimens were wild caught in suburban areas surrounding Alexandra Headland in South-East Queensland, Australia. Field work was conducted from September to October 2018. The specimens were caught using primarily hand foraging, a head torch and clear plastic containers. We did not differentiate between sexes and spiders with less than 8 legs were not excluded from the study, but the effect of limb loss was tested below.

Speed and kinematic measurements on running spiders

To measure maximum speed and movement kinematics, an arena 75 mm wide and 500 mm long was built, with a chip board base and smooth corflute walls. One side of the racetrack was replaced with clear Perspex sheeting, allowing strides to be recorded simultaneously from the side and the top. High-speed cameras positioned laterally to (HiSpec1, Fastec Imaging, San Diego) and directly above (Fastec IL3, Fastec Imaging) recorded views at 250 fps, 1/500 s shutter, and 1280×960 px resolution. Cameras were synchronised using an internal trigger. Lighting was provided using 2×150 W Nelson Clamp floodlight and 4x 'Brilliant Lighting' Photography LED 6 W lights. Two lenses were used, a 28 mm NIKON AF NIKKOR lens F/2.6, and a 90 mm Tamron Macro lens, F/2.8, which were changed in accordance with the size of each specimen. Each spider was encouraged to run at maximal speed three times, by gentle touching with a fine paintbrush to the abdomen. Spiders were allowed to rest between runs, usually for 1–2 min. Runs where the spider was visually fatigued were not included in the analysis. The temperature was controlled throughout all experimental days, ranging from 27 to 28 °C.

Lateral views were analysed in Image J to extract stance and swing phases for each leg (1, 2, 3, 4; Fig. 1b). The timestamps for each leg were recorded as foot fall (FF), end of stance (ES) and subsequent foot fall (SubFF). Stride length was determined using the calibrated view from the dorsal perspective. A landmark at the tip of each leg was digitized in Matlab (version R2019, Mathworks, Inc., Natick, MA) using DLTdv6.m (Hedrick 2008). An additional landmark on the abdomen was used to estimate speed. Instantaneous speed was calculated as the distance
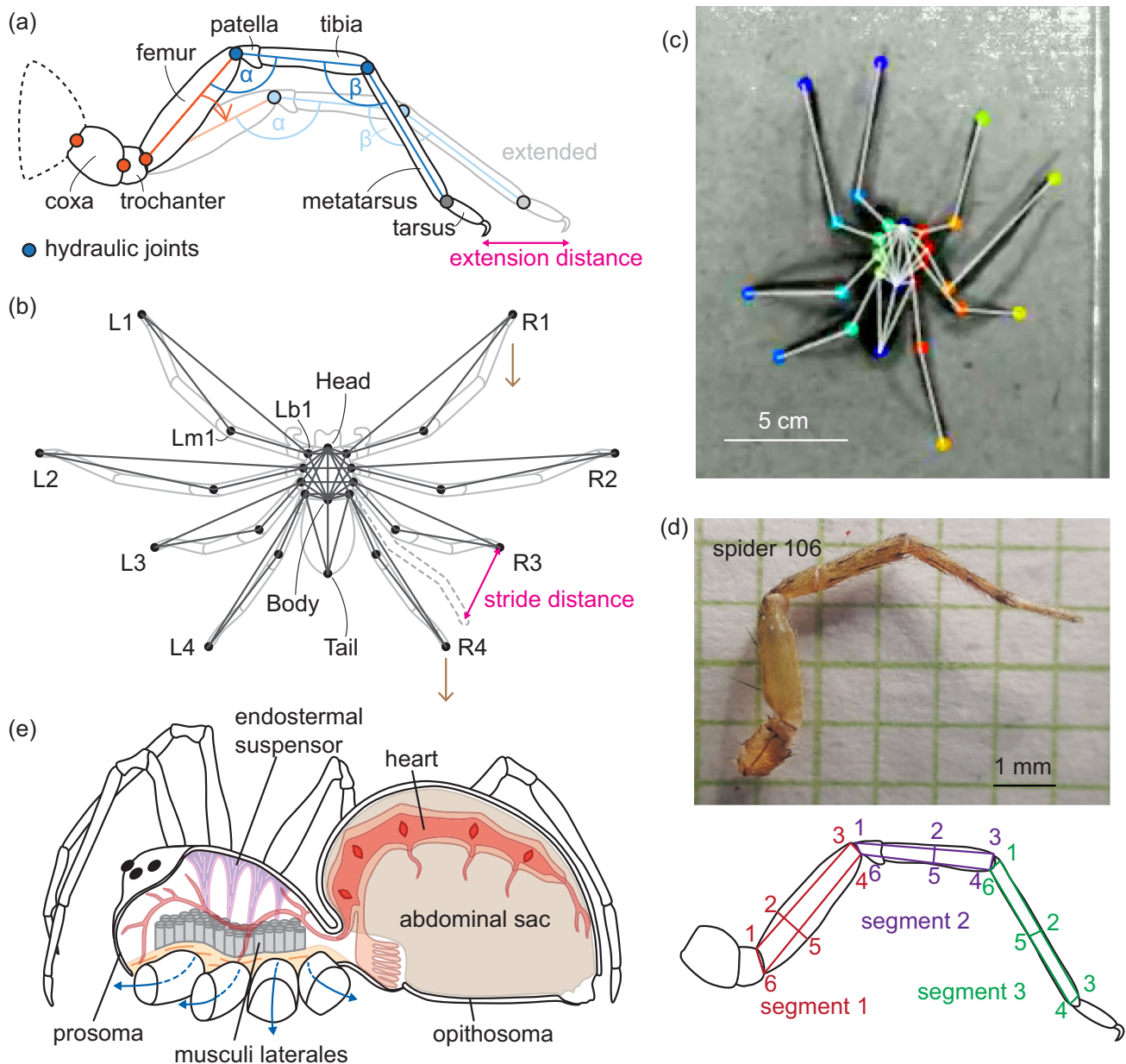
Fig. 1 The mechanics of the leg extension and kinematic and morphometric analysis. **a** The different segments and joints in a spider leg. Joints which are involved in leg extension are highlighted. Orange joints are extended with extensor muscles and blue joints with the hydraulic extension. Leg extension works through femoral depression towards the substrate and an increase of the ventral angles of the femur–patella and the tibia–metatarsal joint. **b** 27 labels and the skeleton which were used to train a deep residual neural network using DeepLabCut and **c** the tracking results, also see Supp. Video 1. **d** displays the definitions of the leg segments used for the morphological analysis of leg length, width and volume. **e** The outline of a general web spider modified after (Kropf 2013). Internal structures/muscles which are relevant for generating hemolymph pressure are displayed

the landmark moved between subsequent frames. The maximum instantaneous speed throughout the stride was used to estimate maximum speed, while the average of all instantaneous speeds was used to calculate mean speed.

Additionally, for a subset of spiders, the positions of spiders and limbs were tracked using the toolbox DeepLabCut (DLC, (Mathis et al. 2018)) for markerless pose-estimation.

A Deep Residual Neural Network (resnet-50) was trained to track 27 tracking points per frame for all videos where the spiders were filmed from a dorsal perspective (Fig. 1b, Supp Video 1). This subset was chosen as the direction of travel (straight-line runs, without touching walls, etc.) facilitated the accuracy of the automatic tracking (Sparassidae $N=27$, $n=77$; Lycosidae $N=39$, $n=117$). The resulting accuracy

after 330,000 iterations of training using the tensor pack image augmentation was 1.38 px train and 3.03 px test error (Fig. 1c), which is close to human accuracy of 2.7 px error (Nath et al. 2019). The output csv files, which contain all coordinates for all labels for every frame and their likelihood, were used to perform several kinematic calculations.

With a custom python script, we extracted flexion and extension phases for each limb using the relative change in distance between the leg tip (tarsus) and the leg base (coxa). All frames with a likelihood < 90% (suggesting lower digitization accuracy) were excluded from analysis. We also calculated the frame-wise distances for the outer leg segment (femoral-patella to tarsus) and the inner leg segment (coxa to femoral–patella joint) for flexion and extension phases to compare the influence of femoral depression and hydraulic extension individually. Within R, all spider runs were then combined using only extension or flexion phases equal to, or greater than, 4 continuous frames.

Morphological analysis

Following the kinematic trials, body masses for all spiders were measured on a Mettler Toledo lab balance (model: PB303-S, error ± 0.5 mg). All spiders were then euthanised by freezing, and four legs from one side of the spider's body were dissected with scalpel blades at the coxa joint. Limbs were photographed from a lateral view on calibrated grid paper using a digital camera OPTUS STYLUS TG-4 in macro format ($n = 504$ legs, $n = 126$ per leg, from $N = 126$ individuals). Images were imported into a custom-built Matlab script, and the field of view was calibrated. The mean length (mm) and mean width (mm) for three main segments: segment 1 (femur), segment 2 (patella + tibia), and segment 3 (metatarsus) (see Fig. 1d) were estimated. Segment width was measured three times for each segment, at the proximal, distal, and mid-shaft section, and the mean value was used for further analysis. Similarly, length was measured on both the dorsal and ventral length of a segment and the mean value used. The volume of each segment was calculated, by assuming a cylindrical shape, following the formula:

$$V = \pi r^2 h, \tag{1}$$

where r was segment width/2 and height approximated segment length.

Statistical analysis

All statistical analyses were run in R studio version 3.5.1 (Feather Spray). The glm.R function from the base package (speed modulation), or the gls.R function, using the maximized-likelihood method (running speeds), from the nlme package in R, was used as described for each analysis

in the results section (Pinheiro et al. 2013). Tukey post hoc tests were then performed using the glht.R function from the multcomp package (Bretz et al. 2016). Confidence intervals (CI) were calculated using the intervals.R function from the nlme package in R. Plots of regression terms against their predictors, with standard errors and partial residuals were produced using the function termplot.R from the stats package in R, based upon models built using the glm function from the base package.

Results

Speed analyses

We ran a generalised linear model comparing maximum stride speed with body mass and family, including the maximum speed recorded for each subject ($N = 128$, 0.0054–3.01 g). We showed a significant effect of mass on running speed among spiders ($F_{1,124} = 334$, $P < 0.001$, Fig. 2a), but no significant effect of family ($F_{1,124} = 0.45$, $P = 0.503$), nor any significant interaction between mass and family ($F_{1,124} = 168$, $P = 0.687$). The combined slope for maximal spider speed was $M^{0.353}$ (95% CI 0.272–0.433).

We ran a similar model, but used mean speed throughout each trial, retrieving the overall mean speed run for each individual. As above, we found a significant effect of mass ($F_{1,124} = 119$, $P < 0.001$), and no effect of family ($F_{1,124} = 0.24$, $P = 0.621$), with a combined slope of $M^{0.197}$ (95% CI 0.107–0.288).

Multiple spiders ($N = 11$) in the dataset did not have all leg pairs. To explore the effect of limb loss on running speed, we calculated residual running speed from mass using the maximal speed model above and compared it with leg number. The number of remaining limbs did not affect running speed among these spiders ($F_{3,372} = 0.411$, $P = 0.745$), at least where the limb number does not decrease lower than 5.

Speed modulation

To explore speed modulation, we measured stride distance and stride duration (stride frequency = 1/stride duration) on a subset of videos ($N = 67$, Mass range 0.0079–3.01 g, Speed range 0.03–1.58 m/s) where limbs could be clearly imaged, and footfalls clearly detected. Among this subset of data, we found a significant effect of mass on speed ($F_{1,63} = 8.29$, $P = 0.005$), no significant effect of family ($F_{1,63} = 1.25$, $P = 0.266$), nor any significant interaction between mass and family ($F_{1,63} = 0.002$, $P = 0.965$). Yet, the slope for this sub-sample of data was lower than maximal speed, but similar to mean speeds, scaling as $M^{0.17}$ (CI 0.005–0.337).

Fig. 2 The scaling of speed with body mass in spiders (**a**) and the termplot for a general linear model of speed modulation techniques, showing partial residuals (**b**, **c**). The speed (m/s) increases with body mass with Mass$^{0.353}$ with Lycosidae (blue dots) and Sparassidae (green dots). Termplots for mass (top row) and family (bottom row) are shown against stride distance (left), stride duration (centre) and duty factor (right). These display partial residuals on the *y*-axis and the focal variable on the *x*-axis together with the corresponding regression line. The slope of the regression line will be identical with the coefficient of the focal variable in the full model
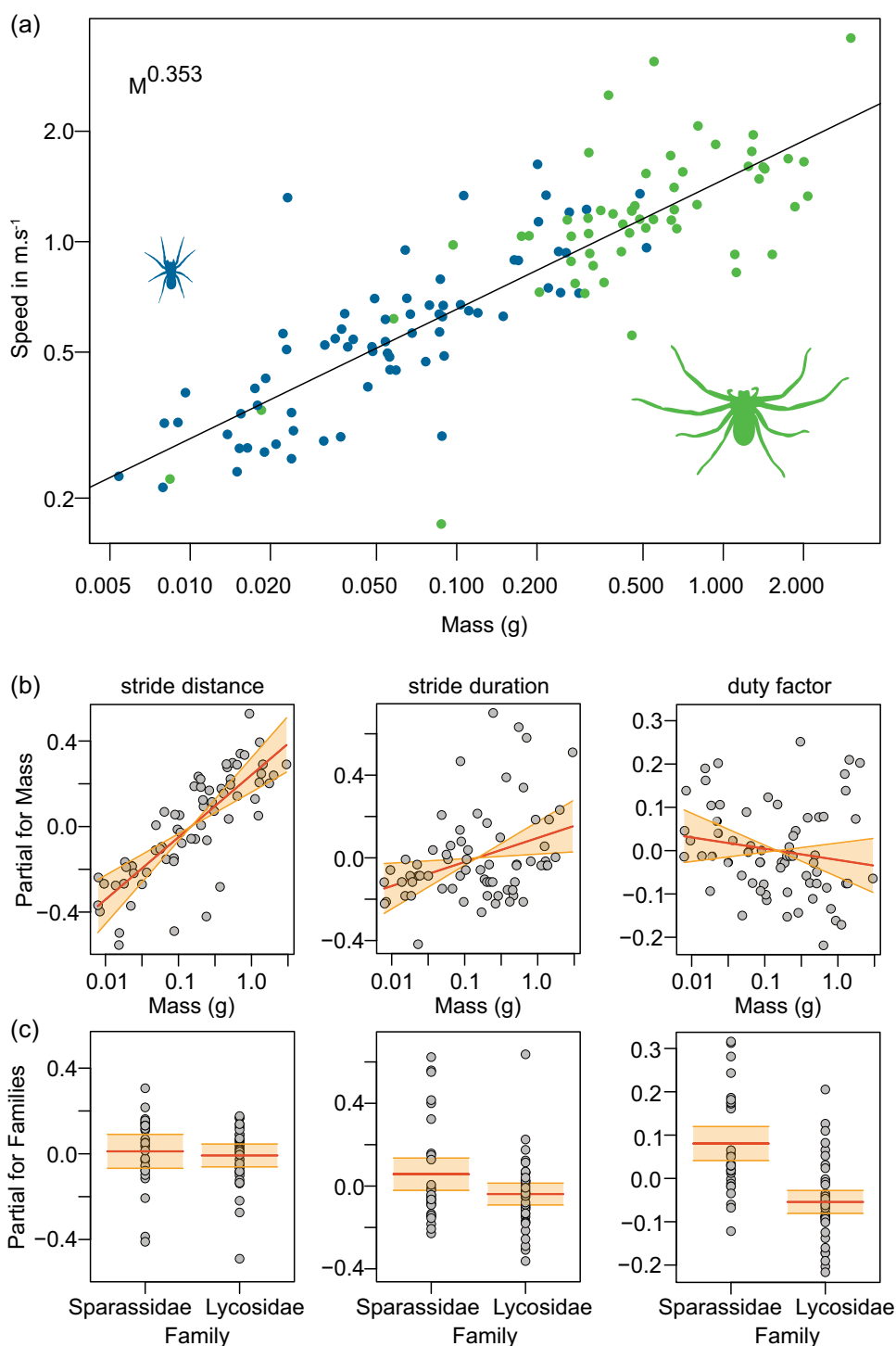
To explore speed modulation among spiders, we measured the straight-line distance between subsequent footfalls for each limb and selected the fastest stride for each individual. Stride distance increased significantly with mass ($F_{1,65} = 131$, $P < 0.001$), but was not significantly different between the families ($F_{1,64} = 0.204$, $P = 0.653$), nor was there any interaction between family and mass ($F_{1,63} = 0.001$, $P = 0.973$). The mean stride distance was 32.83 mm (± 17.96 mm SD). Collectively, the scaling of stride distance was M$^{0.29}$ (95% CI 0.196–0.386).

Along with increasing distance, the duration for each stride also increased with body mass, suggesting larger spiders adopt a lower stride frequency. Stride frequency was significantly associated with mass ($F_{1,65} = 17.7$, $P < 0.001$), but with no effect of family ($F_{1,64} = 2.12$, $P = 0.150$), nor an interaction between these factors ($F_{1,63} = 0.41$, $P = 0.512$).
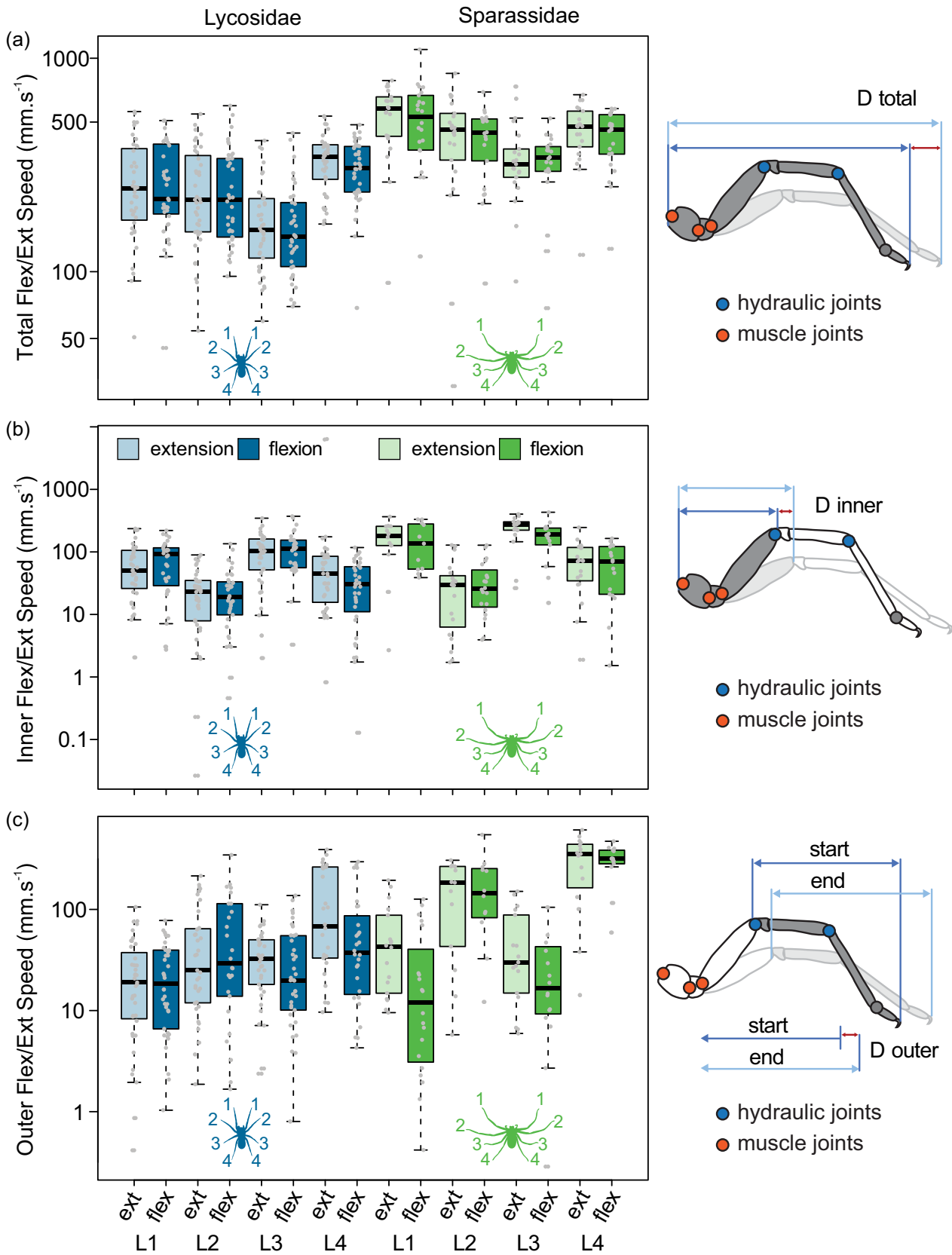
◀**Fig. 3** Flexion and extension speed of different leg segments, separated by family (left, blue—Lycosida; Right, green Sparassidae), and leg number (1—front limbs, 4 hind limbs). **a** Flexion and extension speeds for the entire leg (coxa to tarsus) Slower flexion/extension speeds are observed for leg 3, and highest speeds in leg 1 and 4. No significant difference between the direction of movement can be reported. **b** Flexion extension speeds of the inner leg segments (coxa to femur–patella) with leg 1 and 3 showing higher flexion/extension speeds than legs 2 and 4, but no significant effect of the direction of movement. **c** Flexion extension speeds for the outer segments (femur–patella to tarsus), the pattern from the inner segment seems to be inverted here, with leg 2 and 4 showing higher extension/flexion speeds and leg 1 and 3 lower speeds. A significant effect of direction of movement was found, suggesting slower flexion than extension speeds

The mean stride duration was 0.096 s ($\pm$ 0.078 s SD). Stride frequency scales as $M^{-0.149}$ (CI 0.013–0.285).

Finally, duty factor (the percentage of the stride cycle where the foot was on the ground) was not affected by mass ($F_{1,65} = 3.15$, $P = 0.081$), nor leg number ($F_{1,61} = 1.06$, $P = 0.372$), but there was a significant effect of family ($F_{1,64} = 16.94$, $P < 0.001$), with Sparassidae showing higher duty factors when compared with the Lycosidae. The interaction between mass and family was not significant ($F_{1,63} = 0.332$, $P = 0.567$). The mean duty factor for Sparassidae was 0.36 ($\pm$ 0.16 SD) and for Lycosidae was 0.25 ($\pm$ 0.12 SD). The effect of stride distance, stride duration, and duty factor with mass is displayed in Fig. 2b, and the interaction with families in Fig. 2c.

Analyses on limb flexion and extension

To further explore limb flexion and extension we analysed a subset of our data using only videos in which limb joints could be successfully tracked by the deeplabcut tracking software. This resulted in 15,085 individual flexion/extension events from 61 spiders (Lycosidae = 39, Sparassidae = 22). We aggregated our data by individual, family, leg number, and direction of movement (flexion and extension) selecting the maximum value for the overall movement speed. We recalculated the relationship between speed and body mass among this subset. Again, we found a significant effect of mass on running speed among spiders ($F_{1,479} = 376$, $P < 0.001$), but there was now a significant effect of family ($F_{1,478} = 9.79$, $P = 0.002$), demonstrating that sparassids were faster than lycosids, and a significant interaction between mass and family ($F_{1,477} = 28$, $P < 0.001$). Our combined slope for maximal running speed was $M^{0.341}$ (CI 0.300–0.382).

We first compared the movement between the leg tip and the leg base (tarsus to coxa). This model showed a significant effect of limb ($F_{3,476} = 68$, $P < 0.001$), family ($F_{1,475} = 374$, $P < 0.001$), and mass ($F_{1,474} = 698$, $P < 0.001$), but no effect of the direction of movement ($F_{1,479} = 1.00$, $P = 0.317$). A

Tukey post hoc test suggested that all leg pairs are significantly different from one another, with the exception of leg 1 vs 4 ($Z = 2.53$, $P = 0.054$). Leg 3 appears to show the least amount of extension and flexion, with limbs 1 and 4 showing higher levels (Fig. 3a). Total limb movement speed tended to increase with body mass, where larger individuals showed greater extension and flexion speeds. Finally, limb speed also significantly varied between family, and while Sparassidae showed greater limb extension speeds (Fig. 3a), this appeared to be explained by the on average larger body mass in this group. A post hoc test suggested once body size is accounted for, Lycosidae show relatively faster flexion and extension speeds ($z = -2.22$, $P = 0.0259$).

We then explored the movement speed between the leg base (coxa) to the femoral–patella joint (inner leg segment), which would be primarily driven by the muscle actuated trochanter–femur joint (Figs. 1a, 3, orange joint). As for the total movement speed above, the speed of movement about this joint significantly varied among limbs ($F_{3,411} = 51$, $P < 0.001$), with family ($F_{1,410} = 25$, $P < 0.001$) and with body mass ($F_{1,409} = 79$, $P < 0.001$), but not movement direction ($F_{1,414} = 0.84$, $P = 0.359$). As above, despite Sparassidae showing greater limb extension speeds, once corrected for larger body size in the model, appeared to have relatively lower movement speeds (Fig. 3b). However, the pattern among the limbs appeared to vary from the earlier pattern. A Tukey post hoc test suggested all comparisons between legs showed a significant difference in movement speed, with legs 1 and 3 showing increased speed of movement at this joint, and limbs 2 and 4 showing a reduction (Fig. 3b).

We next explored the movement between the femoral–patella joint and the tarsus (outer leg segment), including the tibial–metatarsal joint—around which flexion is driven by direct muscular contraction, but extension may be primarily driven by the hydraulic system. Here, we report a significant effect of direction ($F_{1,390} = 5.98$, $P < 0.015$), in addition to significant effects of limb ($F_{3,387} = 38$, $P < 0.001$), species ($F_{1,386} = 29$, $P < 0.001$), and mass ($F_{1,385} = 53$, $P < 0.001$). Around this femoral–patella joint, flexion speeds tended to be slower than the extension speeds ($z = -2.35$, $P = 0.018$). Movement speed also varied significantly among all limb pairs with the exception of the comparison between legs 3 and 1. The pattern among the legs appears to the inverse of those at the trochanter–femur joint, with movement speeds being higher for limbs 2 and 4, and lower among limbs 1 and 3 (Fig. 3c). The effect of species becomes weaker when analysed in a post hoc analysis ($Z = -0.47$, $P = 0.638$).

Finally, we examined the interaction between limb and mass in movement speed at each joint to determine if increasing body size was associated with changes in joint use. We found a significant interaction between mass and total extension/flexion speed ($F_{3,472} = 16$, $P < 0.001$), as well as an interaction between mass and leg extension/

flexion speed in the distal joint ($F_{3,383} = 9.5$, $P < 0.001$), but this effect was weaker in the proximal joint ($F_{3,407} = 2.37$, $P = 0.069$). Movement direction did not have a significant interaction in any case. For the total extension/flexion speed limbs 1–3 appear to share a similar slope when plotted against body mass, but limb 4 appears to show a shallow slope, indicative of decreased reliance on this limb in larger individuals (Suppl. Fig. 1, top). For the movement speed among the distal joint, both limbs 2 and 4 show similar steep slopes with body size, while limbs 1 and 3 show much shallower slopes (Suppl. Fig. 1, bottom). The opposite appears to be true for the proximal joint, with legs 1 and 3 showing relatively steep slopes, and limbs 2 and 4 shallow slopes, but this effect is much reduced (Suppl. Fig. 1, middle).

Morphological analyses

We examined limb shape among spiders including log-transformed segment length against log-transformed body mass, with leg number and species as cofactors. Among segments 1–3, length was significantly associated with body mass, leg number, and families ($P < 0.001$ in each case). The slope for length of each segment with mass is given in Table 1 (also see Fig. 4). Among Lycosidae, the length of the segments did not scale differently from the expectation under geometric similarity ($M^{0.33}$); however, higher than expected scaling was suggested for segments 2 + 3 among Sparassidae, suggesting that these segments get relatively longer in larger bodies individuals. A Tukey post hoc test suggests the significant effect of species results from the longer lengths of all segments among Sparassidae compared with Lycosidae. Finally, the pattern among legs is complex. Tukey post hoc test for models which exclude interaction effects suggests that Segment 1–3 are longest in leg 4 and shortest in leg 3, with legs 1 and 2 showing intermediate lengths (Suppl. Figs. 2, 3, 4).

Unlike for limb lengths above, while body mass and leg number did have a significant effect on segment width ($P < 0.001$ in each case), there was no significant difference between species. Among Lycosa, the segment width again followed the expected scaling under geometric assumptions, while among Sparassidae, the segments widths tended to scale higher than expected. Patterns among the legs were consistent with the widest segments being present in legs

Table 1 Scaling exponents of linear models for log-transformed segment lengths and width with log-transformed body mass in two species of spiders

	Length			Width			Volume		
	Est	2.5%	97.5%	Est	2.5%	97.5%	Est	2.5%	97.5%
Lycosidae									
Seg 1	0.354	0.327	0.381	0.325	0.304	0.346	1.004	0.938	1.071
Seg 2	0.357	0.328	0.386	0.313	0.291	0.335	0.984	0.915	1.053
Seg 3	0.369	0.325	0.413	0.320	0.293	0.346	1.009	0.922	1.095
Sparassidae									
Seg 1	0.338	0.304	0.372	0.356	0.341	0.370	1.055	1.001	1.109
Seg 2	0.359	0.340	0.378	0.347	0.331	0.362	1.053	1.008	1.097
Seg 3	0.367	0.344	0.390	0.353	0.339	0.367	1.074	1.035	1.112

Scaling is also shown for estimated volumes of leg segments assuming a cylindrical shape for each segment

Fig. 4 Showing the scaling of segments lengths and widths in mm for the three leg segments for both families. Both families showed segment 3 to be shortest, and segment 1 to be the longest, while the segments decreased gradually in width from segment 1–3. Both segment lengths and widths increased with body mass. Slopes are listed in Table 1
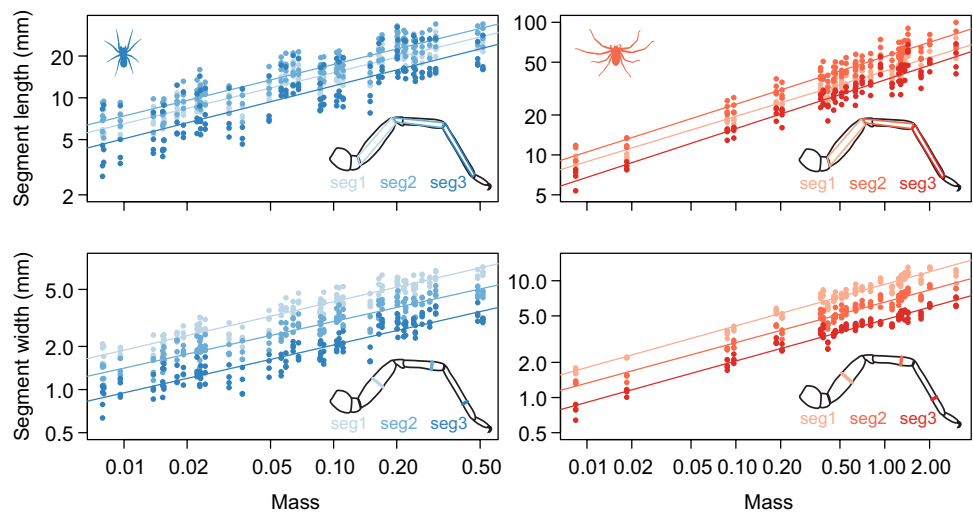
1 and 4, and the shortest appearing in leg 2 (Suppl. Figs. 2, 3, 4).

Combining these measures together suggests that Sparassidae have relatively larger volume limb segments which scale higher than expected under geometric similarity. Among segments 1–3, predicted volume was significantly associated with Mass, leg and Species ($P < 0.001$ in each case). The pattern among the legs also mirrored the results above, with leg 4 showing relatively larger volumes, particularly in segments $1 + 3$. In segment 2, leg 1 also shows a higher predicted volume, with legs $2 + 3$ tending to be consistently smaller (Suppl. Figs. 3).

Discussion

Spiders are unique among terrestrial legged animals in that the power for locomotion is achieved through a combination of direct muscular shortening of muscles which span across joints, and through changes in the internal hydraulic pressure of the prosoma which extends distal joints (Parry and Brown 1959; Weihmann et al. 2012). To understand how this system may affect running speed, we explored the escape speed of 128 spiders, of 2 different families ranging over 3 magnitudes in body mass (0.0054–3.01 g) and found that maximum speed scales with Mass$^{0.353}$. This result is much higher than reported by Hirt et al. (2017) who examined the exploratory speed of 57 species of invertebrates, where speed scaled with Mass$^{0.19}$. However, the scaling of speed varies significantly with taxon, and among the 16 of the 57 species which were of the class Arachnida, speed scaled with Mass$^{0.43}$, which is higher than our current reported scaling. Yet, if we further separate at order and include only the 9 species of the order Araneae (0.0014–0.1084 g), speed scales with Mass$^{0.327}$, much closer to our reported slope. This supports the assertion by Hirt et al. (2017) that differences in the scaling among taxonomic groups are significantly large, and likely arise from differences in the body shape and other traits associated with locomotion, and further research would be required to understand its functional significance.

We also explored the mean running speed and found a much lower scaling exponent of M$^{0.197}$, which is now similar to the average scaling exponent across all six taxonomic groups (M$^{0.19}$) or to the taxon Insecta (M$^{0.19}$) (Hirt et al. 2017), or even to the speed scaling in lizards (M$^{0.18}$) (Van Damme and Vanhooydonck 2001). Similarly, in our sub-setted data, ranging over three orders of magnitude of body mass to explore speed modulation (where selection of maximal speed stride is unlikely to occur frequently), we found that maximum running speed now scaled with M$^{0.17}$. This suggests that the use of maximal speeds may be

relatively uncommon, and these lower scaling exponents may be more ecologically relevant.

Speed modulation strategies revealed remarkable similarities to those reported for mammals, which suggested a scaling of stride frequency of M$^{-0.14}$ and a scaling of stride length of M$^{0.38}$ at equivalent points of gait (Heglund and Taylor 1988). Among spiders as size increases, stride length increases more rapidly (M$^{0.29}$) than the decreases in stride frequency (M$^{-0.15}$), such that larger spiders generally move faster. While the increases in stride length can be explained by near geometric increases in limb length (Fig. 4, Suppl. Figs. 2), the decreases in stride frequency appear to follow similar patterns to those predicted by dynamic similarity $\sim M^{-1/6}$, suggesting similar constraints may be present among diverse lineages (Alexander 1984, 2004; Alexander and Jayes 1983). Similarly, the stride frequencies here appear (range ~ 2.55–35.7 Hz at 28 °C) to be much similar to those of reported among other groups.

Reported cycle frequencies for weight-bearing locomotory muscles of terrestrial animals are similar. Lizard and mouse fast-twitch fibers attain frequencies of 25–30 Hz at 35 °C (Rome and Lindstedt 1998), and cockroach leg muscles cycle at a comparable range during running (15–27 Hz at 23–26 °C) (Full and Tu 1991). Previous studies on stride frequencies in wolf spiders reported that the range of frequencies reported for *Trochosa ruricola* and *Lycosa tarentula* were between 4 and 16 Hz (Ward and Humphreys 1981). The higher frequencies reported in the current study (max 35.7 Hz) are probably a result of the inclusion of smaller bodied spiders. For example, the highest stride frequencies have been reported for the two small bodied North American erythracarid mites which use stride frequencies up to 80–100 Hz (Wu et al. 2010). This pattern of stride frequency suggests no constraint of the hydraulic system in spiders.

We hypothesized that if the hydraulic system was limiting speed, then the extension speed of the hydraulic joints may be slower in bigger spiders, since increases in volume scale faster than the cross section area of muscles, yet our results show an opposite trend. We found that the flexion speed in the outer leg segment, where extension is driven by hydraulic pressure, were slower than the extension speed, whereas we found no significant difference between extension and flexion speeds in the inner leg segment, where both extension and flexion are driven by leg muscles which cross these joints.

Instead, this seems to agree with models of the hydraulic system which include rates of flow. We modelled the hydraulic system based on the Poiseuille equation which relates the flow rate of a fluid through a pipe (Q) to the diameter (d), the pressure difference (ΔP), the viscosity (μ), and length (l) of the system based on Eq. 2.

$$Q = \frac{\pi d^4 \Delta P}{8 l \mu}. \tag{2}$$

For a purely geometric system, we would expect both diameter and length to scale as $M^{0.33}$, while no scaling might be expected for viscosity. This means that the rate of fluid flow (Q) would be equal to $(M^{0.33})^4$. $\Delta P/M^{0.33}$, or $Q = M^1$. ΔP, meaning that the rate of flow would depend on the change in pressure. Based upon Kropf (2013), hemolymph pressure in the legs is increased by the activity of the heart, and by both the musculi laterals and the endosternal suspensor muscles situated in the opithsoma and prosoma (Fig. 1e). Therefore, changes in the pressure between the limbs and the prosoma would depend on the cross-sectional area of muscle which is expected to scale as $M^{0.66}$. Similarly, the flexor muscles, which actuate joints in the limbs, might also be expected to scale with cross-sectional area ($M^{0.66}$), meaning that both systems might maintain similar functionality as body size increased, if they acted independently. However, this is not the case. The hydraulic system functions to produce a high constant pressure, which would tend to constantly extend limb joints. This may limit the action of the flexor muscles, which have to counteract the resting hydraulic pressure always apparent in spiders plus the activity pressure, which can be up to $50 \times$ higher (Kropf 2013; Parry and Brown 1959), explaining the reduction in flexion speed.

Our near geometric scaling of segment lengths appears to support this model (Table 1). Among Sparassidae, the mean scaling of length was $M^{0.35}$, while mean width (which should approximate diameter) scales as $M^{0.35}$ which would result in a scaling of $M^{1.00} \Delta P$. Only among Lycosidae might there be a slight decrease in flow as the mean scaling of length was $M^{0.36}$ while width scales as $M^{0.32}$ which would result in a scaling of $M^{0.92} \Delta P$. Yet in both cases, if the change in pressure increases with muscle cross-sectional area, we might than expect the rate of flow to be greater than the increase in body mass.

However, changes in the hydraulic system may be much more subtle than previously thought. Among Texan brown tarantulas (*Aphonopelma hentzi*, previously known as *Eurypelma californicum*), with a body mass of 15.5 g, stride frequency continued to increase with speed and temperature (Booster et al. 2015). Yet, the proximal and distal hydraulically extended, in-series joints of the forelegs and hindlegs were less tightly coupled, which suggests that increased stride frequency may limit the time available for hemolymph to flow completely into and out of the leg (Booster et al. 2015). Further, among Rose haired tarantulas (*Grammostola rosea*, Mass ~ 30 g), the hydraulically driven femur–patella and tibia–metatarsus joints showed widely varying angles when walking up sloped soft pavement (Hao et al. 2019).

We further hypothesized that the role of the different legs could be reflected in the changes to flexion and extension speeds. Given the radial arrangement of limbs the first and second limbs flex to produce propulsion, while the third limb with its medial orientation would move at its proximal joint. Only the hindlimb with its rearward orientation might be limited by the need to propel the body forward using the hydraulic system (Weihmann et al. 2012). Our results support this pattern in the third limb, which consistently showed reduced flexion and extension in the distal joints suggesting an increased role of the proximal joint; however, the role of the other limbs was more complex. Neither the front nor the hind limbs show significant differences in extension and flexion speeds suggesting, as discussed above, that the two systems show similar abilities to both flex and extend the limb. However, two patterns did emerge among limb use; the alternating pattern of joint use among limbs (Fig. 3b, c) and a reduced movement speed in the rearward facing fourth limb with size (Suppl. Fig. 1).

The pattern of joint use along each limb appeared to vary, such that adjacent limbs showed differing patterns. Specifically, movement at the trochanter–femur joint seems to be largest for limbs 1 and 3, but reduced in limbs 2 and 4. Alternatively movement at the distal joints show an inverse pattern, with greater movement in limbs 2 and 4 compared with 1 and 3 (Fig. 3b, c). Furthermore, this pattern seems to be accentuated at larger body sizes (Suppl. Fig. 1). This may represent a strategy to avoid interference with adjacent limbs during running. The pattern of leg movement in spiders is characterised by the use of two alternative groups of limbs; limbs 1 and 3 on the left side combined with 2 and 4 on the right and vice-versa, though variation in this pattern may exist (Biancardi et al. 2011; Spagna et al. 2011; Ward and Humphreys 1981; Wilson 1967) (Supp. Fig. 5). Differential joint flexion/extension may then allow foot placement to be separated along the medial–lateral axis, and reduce collision between adjacent limbs, though this needs to be confirmed with further kinematic study. Similar results have also been described for the large Central American spider *Cupiennius salei* (Weihmann 2013).

The reduced movement in the rearward facing hindlimbs with body size appears to differentiate this limb from the three others, suggesting that the contribution to propulsion of this limb is reduced in larger bodied spiders. Yet, this reduction does not appear to be strongly linked with a limit to the hydraulic system as there appears to be no significant difference in flexion and extension speeds. This pattern can be observed in high-speed videos where larger bodies spiders appear to passively drag the hindlimbs along behind the body and rely more heavily on the forelimbs for propulsion (Supp. Video 2, 3). This dragging behaviour has been reported in the other studies before, where it was proposed that it could be caused by

the spiders' dragline silk, which may pull the hind legs and abdomen down (Spagna et al. 2011; Ward and Humphreys 1981). Yet, silk drag lines were not clearly apparent in our videos (Supp. Videos 1, 2, 3).

Instead, an alternative explanation for this pattern may be the increased size of the abdomen in larger spiders. While it is unclear how relative abdomen size scales with body mass, the cranial/forward distribution of the limbs likely limits their ability to lift the abdomen off the ground, e.g., see Fig. 1 in (Weihmann et al. 2015). The scaling of segment length appears to show that spiders attempt to compensate for this with relatively longer lengths and diameters, particularly in the most distal segment—which would help to place the supporting limb more distally under the abdomen (Suppl. Fig. 2, 3, 4). However, the ability of the hindlimbs to support this added mass appears to be reduced in the largest spiders, which results in both the hindlimbs and the abdomen being dragged along the ground (Supp. Video 3). This would likely limit further increases and running speed and may ultimately limit body size, at least within these families. How spiders from larger bodied families solve this problem, either through relatively longer limbs, or by changes in the ratio of the prosoma to abdomen, remains to be resolved.

Declarations

Conflict of interest The authors declare no conflicts of interest.

Ethics approval All applicable international, national, and/or institutional guidelines for the care and use of animals were followed.

Consent for publication All authors have indicated consent for publication.

References

Alexander RM (1984) The gaits of bipedal and quadrupedal animals. Int J Robot Res 3:49–59

Alexander RM (2004) Bipedal animals, and their differences from humans. J Anat 204:321–330

Alexander RM, Jayes A (1983) A dynamic similarity hypothesis for the gaits of quadrupedal mammals. J Zool 201:135–152

Anderson J, Prestwich K (1975) The fluid pressure pumps of spiders (Chelicerata, Araneae). Zeitschrift für Morphologie der Tiere 81:257–277

Bejan A, Marden JH (2006) Unifying constructal theory for scale effects in running, swimming and flying. J Exp Biol 209:238–248

Biancardi CM, Fabrica CG, Polero P, Loss JF, Minetti AE (2011) Biomechanics of octopedal locomotion: kinematic and kinetic analysis of the spider *Grammostola mollicoma*. J Exp Biol 214:3433–3442

Biewener A, Daniel T (2010) A moving topic: control and dynamics of animal locomotion. The Royal Society, London

Blickhan R, Barth FG (1985) Strains in the exoskeleton of spiders. J Comp Physiol A 157:115–147

Bohmann L, Blickhan R (1998) Der hydraulische mechanismus des spinnenbeines und seine anwendung für technische probleme. ZAMM J Appl Math Mech 78:87–96

Booster N, Su F, Adolph S, Ahn A (2015) Effect of temperature on leg kinematics in sprinting tarantulas (*Aphonopelma hentzi*): high speed may limit hydraulic joint actuation. J Exp Biol 218:977–982

Bretz F, Hothorn T, Westfall P (2016) Multiple comparisons using R. CRC Press

Clemente CJ, Thompson G, Withers P (2009) Evolutionary relationships of sprint speed in Australian varanid lizards. J Zool 278:270–280

Ehlers M (1939) Untersuchungen über Formen aktiver Lokomotion bei Spinnen. Fischer

Ellis C (1944) The mechanism of extension in the legs of spiders. Biol Bull 86:41–50

Full RJ, Tu MS (1991) Mechanics of a rapid running insect: two-, four-and six-legged locomotion. J Exp Biol 156:215–231

Garland T (1983) The relation between maximal running speed and body mass in terrestrial mammals. J Zool Lond 199:157–170

Garland T, Losos JB (1994) Ecological morphology of locomotor performance in squamate reptiles. In: Wainwright PC, Reilly SM (eds) Ecological morphology: integrative organismal biology. University of Chicago Press, Chicago, pp 240–302

Gasparetto A, Vidoni R, Seidl T (2008) Kinematic study of the spider system in a biomimetic perspective. In: 2008 IEEE/RSJ International Conference on Intelligent Robots and Systems. IEEE, pp 3077–3082

Hao X, Ma W, Liu C, Li Y, Qian Z, Ren L, Ren L (2019) Analysis of Spiders' joint kinematics and driving modes under different ground conditions. Appl Bionics Biomech

Hedenström A (2003) Scaling migration speed in animals that run, swim and fly. J Zool 259:155–160

Hedrick TL (2008) Software techniques for two-and three-dimensional kinematic measurements of biological and biomimetic systems. Bioinspir Biomim 3:034001

Heglund NC, Taylor CR (1988) Speed, stride frequency and energy cost per stride: how do they change with body size and gait? J Exp Biol 138:301–318

Heglund NC, Taylor CR, McMahon TA (1974) Scaling stride frequency and gait to animal size: mice to horses. Science 186:1112–1113

Hirt MR, Lauermann T, Brose U, Noldus LP, Dell AI (2017) The little things that run: a general scaling of invertebrate exploratory speed with body mass. Ecology 98:2751–2757

Iriarte-Díaz J (2002) Differential scaling of locomotor performance in small and large terrestrial mammals. J Exp Biol 205:2897–2908

Kropf C (2013) Hydraulic system of locomotion. Spider ecophysiology. Springer, Berlin, pp 43–56

Mathis A, Mamidanna P, Cury KM, Abe T, Murthy VN, Mathis MW, Bethge M (2018) DeepLabCut: markerless pose estimation of user-defined body parts with deep learning. Nat Neurosci 21:1281–1289

Nath T, Mathis A, Chen AC, Patel A, Bethge M, Mathis MW (2019) Using DeepLabCut for 3D markerless pose estimation across species and behaviors. Nat Protoc 14:2152–2176

Parry D, Brown R (1959) The hydraulic mechanism of the spider leg. J Exp Biol 36:423–433

Pennycuick C (1997) Actual and 'optimum' flight speeds: field data reassessed. J Exp Biol 200:2355–2361

Peters RH (1986) The ecological implications of body size, vol 2. Cambridge University Press, Cambridge

Petrunkevitch A (1909) Contributions to our knowledge of the anatomy and relationships of spiders. Ann Entomol Soc Am 2:11–21

Pinheiro J, Bates D, DebRoy SS, Sarkar D (2013) Nlme: linear and nonlinear mixed effects models R package version 31-110 3:1–113

Rome LC, Lindstedt SL (1998) The quest for speed: muscles built for high-frequency contractions. Physiology 13:261–268

Spagna JC, Valdivia EA, Mohan V (2011) Gait characteristics of two fast-running spider species (*Hololena adnexa* and *Hololena curta*), including an aerial phase (Araneae: Agelenidae). J Arachnol 39:84–91

Van Damme R, Vanhooydonck B (2001) Origins of interspecific variation in lizard sprint capacity. Funct Ecol 15:186–202

Ward T, Humphreys W (1981) Locomotion in burrowing and vagrant wolf spiders (Lycosidae). J Exp Biol 92:305–321

Weihmann T (2013) Crawling at high speeds: steady level locomotion in the spider *Cupiennius salei*—global kinematics and implications for centre of mass dynamics. PLoS ONE 8:e65788

Weihmann T, Günther M, Blickhan R (2012) Hydraulic leg extension is not necessarily the main drive in large spiders. J Exp Biol 215:578–583

Weihmann T, Goetzke HH, Günther M (2015) Requirements and limits of anatomy-based predictions of locomotion in terrestrial arthropods with emphasis on arachnids. J Paleontol 89:980–990

Wilson DM (1967) Stepping patterns in tarantula spiders. J Exp Biol 47:133–151

Wu GC, Wright JC, Whitaker DL, Ahn AN (2010) Kinematic evidence for superfast locomotory muscle in two species of teneriffiid mites. J Exp Biol 213:2551–2556